Changes in Cadmium Telluride Photovoltaic System Performance due to Spectrum

Lauren Nelson, Mark Frichtl, and Alex Panchula

***Abstract*—Seasonal and short-term weather-related changes in the solar spectrum can induce shifts in the performance of photovoltaic (PV) systems that affect both annual energy predictions and system characterization. The spectral shift factor, which is a metric indicative of how much the performance of a PV system will vary from nameplate due to deviations from the ASTM G173 spectrum (air mass of 1.5), is predicted using TMY3 data and the simple model of the atmospheric radiative transfer for sunshine (SMARTS) model and is correlated with cadmium telluride (CdTe) PV system performance in four different climates. The predicted spectral shift factors for CdTe systems show improved performance in the late summer and early fall and diminished performance in the winter. These intraannual variations can be as large as ± 3%, but annual spectral shift factors are typically within ± 1% of nameplate. The spectral shift factor of CdTe systems was found to be most sensitive to the precipitable water content of the atmosphere. Consequently, a parameterization of CdTe spectral shift factor as an exponential function of precipitable water is derived using the outputs of the SMARTS model in 11 locations. This parameterization is shown to predict observed monthly and daily fluctuations in CdTe PV performance. Future efforts will incorporate this methodology into energy predictions that will reduce uncertainty.**

***Index Terms*—Cadmium telluride (CdTe), modeling, photovoltaic (PV) systems, spectrum.**

I. Introduction

THE effects of changes in the distribution of incident light spectrum on photovoltaic (PV) system field performance have been reported to be smaller than 3% in general and larger for thin films than traditional crystalline silicon (c-Si) [1]. Many commercially available PV system simulation tools do not include a spectral model, which introduces additional uncertainty into energy predictions [11]–[13]. Seasonal fluctuations are studied using an atmospheric spectral irradiance model and actual PV system performance in a wide variety of climates. A simple parameterization of modeled spectral fluctuations for cadmium telluride (CdTe) systems is offered and validated against measured system performance.

II. Spectral Shift Factor

Spectral responsivity (SR) is the percent of available radiant power that a PV device converts into current (units are A/W) as a function of the wavelength of incident light. SR is directly related to the quantum efficiency QE—the number of charge carriers that are generated per incident photon of a given wavelength—of a device

$$\mathrm{SR}_\lambda = \mathrm{QE}_\lambda \cdot \lambda \cdot \frac{e}{hc} \tag{1}$$

where e is the fundamental charge, h is Plank's constant, and c is the speed of light.

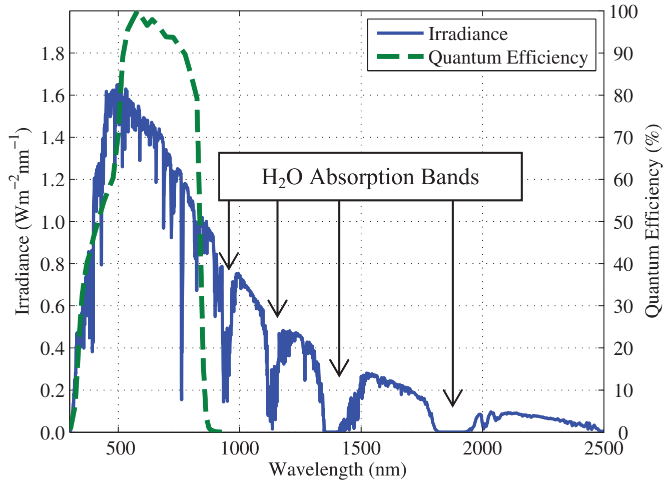

Fig. 1. Global irradiance spectrum defined by ASTM G173 and an example QE curve normalized to 100% for a CdTe PV cell.

A QE curve for CdTe that is normalized to 100% is shown in Fig. 1. The range of operation for CdTe is approximately 280–900 nm, while a broadband device such as a thermopile pyranometer has a theoretical SR of 100% from 280 to 3000 nm, and is, therefore, resilient to changes in spectrum.

The solar spectral irradiance distribution (also shown in Fig. 1) describes light intensity as a function of wavelength. The reference spectral irradiance distribution under which PV module nameplate ratings are defined is given by the global spectrum in ASTM G173, which is considered to be a representative of the average spectrum in the 48 contiguous United States [4]. A number of input variables are used to derive ASTM G173 such as a tilt of 37°, a precipitable water vapor column of 1.42 cm, and an absolute air mass of 1.5 (AM1.5) which corresponds to a solar zenith angle of 48.19°. Note that with regard to PV modules and systems, ASTM G173 is commonly referred as AM1.5, which is just one of the many variables used to define it.

The measured spectral irradiance distribution varies as a function of time of day, season, and location, among other variables. When coupled with a PV QE curve, these shifts can have significant effects on PV system performance. Atmospheric

Manuscript received May 21, 2012; revised September 25, 2012; accepted October 14, 2012. Date of publication November 19, 2012; date of current version December 19, 2012.

The authors are with First Solar, San Francisco, CA 94105 USA (e-mail: Lauren.Nelson@firstsolar.com; markfrichtl@gmail.com; APanchula@firstsolar.com).

Color versions of one or more of the figures in this paper are available online at http://ieeexplore.ieee.org.
Digital Object Identifier 10.1109/JPHOTOV.2012.2226868

constituents such as carbon dioxide, oxygen, and water absorb light at different wavelengths. The majority of the absorption bands outside of the CdTe QE can be attributed to water vapor absorption, as labeled in Fig. 1. There are some narrow water vapor absorption bands within the CdTe QE, but the reduction of light transmittance is smaller in these bands than in those outside of the CdTe QE. Absorption bands due to other atmospheric constituents (CH_4, CO, CO_2, N_2, N_2O, O_2, and O_4) are narrower at atmospheric temperature and pressure than those due to H_2O and, therefore, less significant in this analysis [2], [3].

The spectral shift factor M is a metric indicative of how much the performance of a PV system will vary from nameplate due to deviations from ASTM G173 [14]. M is defined as the ratio of irradiance-specific current produced under an arbitrary spectrum to the irradiance-specific current produced under G173 [17]. When the irradiance sensor against which the plant performance is being assessed has a constant SR versus wavelength (as in the case of a thermopile pyranometer, but not a PV reference cell or module), M is given by

$$M = \frac{\int E(\lambda) \cdot \mathrm{SR}(\lambda) d\lambda}{\int E(\lambda) d\lambda} \cdot \frac{\int E_{G173}(\lambda) d\lambda}{\int E_{G173}(\lambda) \cdot \mathrm{SR}(\lambda) d\lambda} \qquad (2)$$

where SR is the responsivity of the PV device as defined in (1), and E is the spectral irradiance under consideration. A value of M greater than 1 indicates irradiance-weighted power output in excess of that at G173. Conversely, a value of M less than 1 indicates irradiance-weighted power output less than that at G173.

The primary goal of this analysis is to quantify the range of M over various climates and seasons, and compare these values of M to observed variations in CdTe PV system performance.

III. Simple Model of the Atmospheric Radiative Transfer for Sunshine Model

The simple model of the atmospheric radiative transfer for sunshine (SMARTS) is an atmospheric model that predicts the spectrum under clear sky conditions. SMARTS requires a number of inputs, which include but are not limited to latitude, longitude, ambient temperature, pressure, and precipitable water. Many of these inputs are available on an hourly basis in TMY3 data files, which are indicative of typical meteorological conditions in a given location [5]. The output of the SMARTS model is a matrix of wavelength and spectral intensity.

To create site-specific SMARTS input files, TMY3 data were first filtered to only include data points, where irradiance was greater than 500 W/m^2 in high-irradiance climates and greater than 300 W/m^2 in temperate climates. This filtering was applied in order to increase computation speed and remove low-energy production hours with high air mass that may skew results. The SMARTS model was then used to simulate a spectrum at all hours that passed the irradiance filter for a given site. Hourly values of M were calculated by using the CdTe QE curve and the outputs of the SMARTS model as inputs to (2). These hourly values were then consolidated into irradiance-weighted monthly averages. The resulting monthly spectral shift factors for Phoenix, AZ, are shown in Fig. 2.

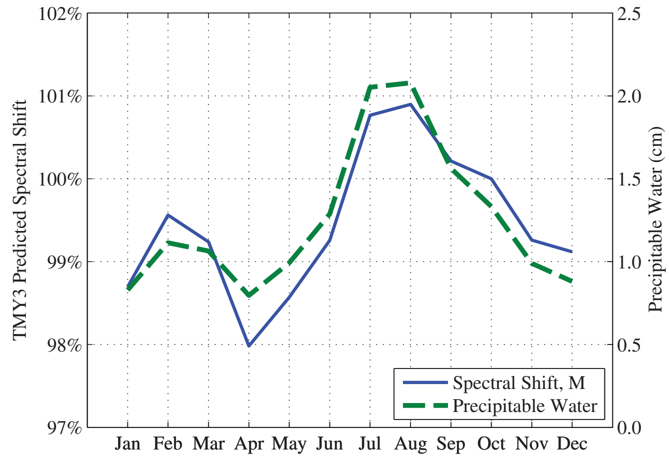

Fig. 2. Monthly spectral shift factors M for CdTe calculated using SMARTS and TMY data with precipitable water content in Phoenix, AZ.

The minimum predicted M for Phoenix occurs in April and is 98.0% (which represents a performance deficit due to a spectrum of 2.0% when compared with nameplate). The maximum M in this location occurs in August and has a magnitude of 100.9%. The irradiance-weighted annual M for this location is 99.5%.

While this type of analysis provides insight into average seasonal changes, its major limitation is that it is only a representative of clear sky days and does not account for spectral effects due to clouds. It is also based on multiyear averages from TMY3 files; therefore, behavior in a single year may deviate significantly from this model.

To assess the magnitude of these effects, the SMARTS method to predict spectral shift factors was compared with the same method applied to measured spectral data. An EKO MS-700 spectroradiometer is mounted in a horizontal orientation in Phoenix, AZ. It collects data between 300 and 1143 nm every 10 min, starting in November 2010. Spectral shift factors for CdTe are calculated every 10 min using (2). To account for the limited spectral range of the measurement device, all integrals in this exercise are evaluated numerically between 300 and 1143 nm (rather than the full range of the broadband device). The monthly median M is calculated and plotted in Fig. 3, along with M predicted using TMY3 data and the SMARTS model.

The relative trend of the measured M is mostly consistent with that predicted using the SMARTS model and TMY data, with better performance in the late summer and diminished performance in the winter. Monthly differences between measured and predicted may be caused by the use of a multiyear average for the prediction or uncertainty introduced by the evaluation of integrals only between 300 and 1143 nm in this exercise. Note that for the remainder of the work presented in this paper, integrals were evaluated between 300 and 4000 nm (limits of the SMARTS model output).

IV. Sensitivity Analysis

The Golden, CO, TMY3 data were filtered to only include hours with irradiance greater than 300 W/m^2. A random sample of 10% of these hours was then generated for use as a proxy

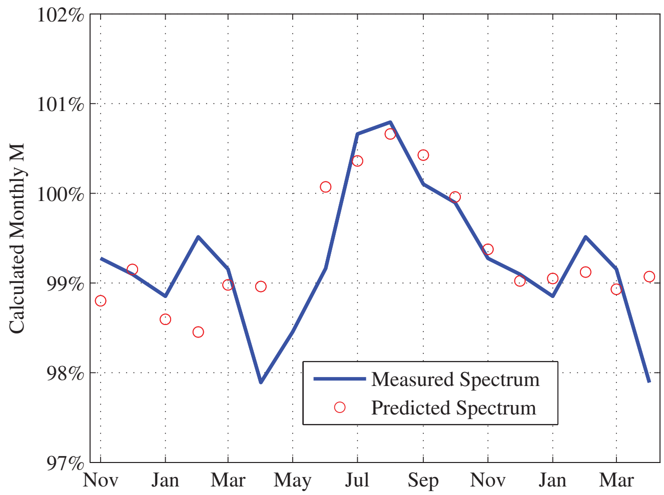

Fig. 3. Monthly spectral shift factors calculated using measured spectral data and spectra generated using SMARTS/TMY3 for Phoenix, AZ, in the horizontal plane.

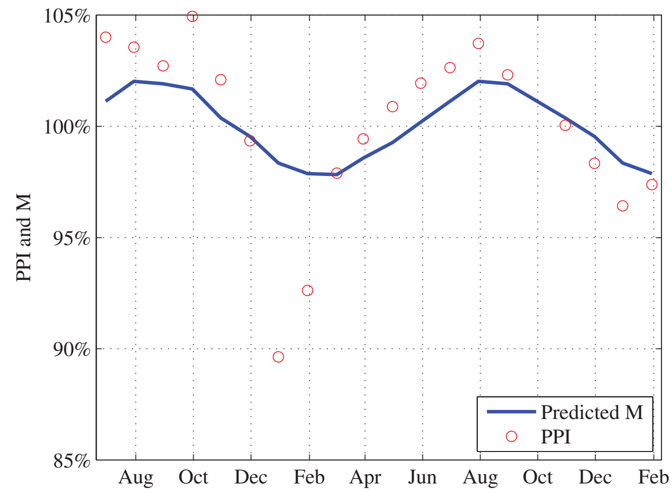

Fig. 4. SMARTS-predicted spectral shift factors and -measured CdTe PV system PPIs in a temperate climate.

TABLE I
SENSITIVITY OF M TO SELECT INPUT PARAMETERS

Variable	Range	Magnitude of effect on CdTe M
Tilt	0° - 45°	± 0.15%
Pressure	750 mbar - 900 mbar	± 0.2%
Aerosol Optical Depth	0.01 - 1	± 0.9%
Ozone Columnar Abundance	0.2 atm-cm - 0.5 atm-cm	± 0.4%
Precipitable Water Content	0.1 cm - 10 cm	± 6%

for the full filtered dataset. For each hour in the sample, the SMARTS model was run many times, varying a single-input parameter at a time. This allowed M to be calculated for each input parameter as a function of timestamp and that input parameter. By irradiance weighting and averaging each M over time, the dependence on time can be removed, resulting in annual M as a function of the variable in question. Table I summarizes the results of the sensitivity analysis. Only parameters that substantially affected M are reported.

The strong dependence of M on precipitable water content P_{wat} (see Figs. 2 and 8) arises from water vapor's absorptivity being highly wavelength dependent over the 280–3000 nm range. Water vapor has very low absorptivity in the wavelengths at which the CdTe QE is high (it is virtually transparent), while its absorptivity in the 900–3000 nm range is considerable [7], [8]. Therefore, given two points in time with identical irradiance as measured by a broadband pyranometer, the time with higher P_{wat} will have a larger fraction of its irradiance fall within the CdTe QE curve than the time with lower P_{wat}. This leads to a strong positive correlation between P_{wat} and M for CdTe, which we discuss in Section VII. This correlation will not be as strong for other PV technologies with different bandgaps. For example, the c-Si QE typically spans from 300 to 1200 nm and will be less sensitive

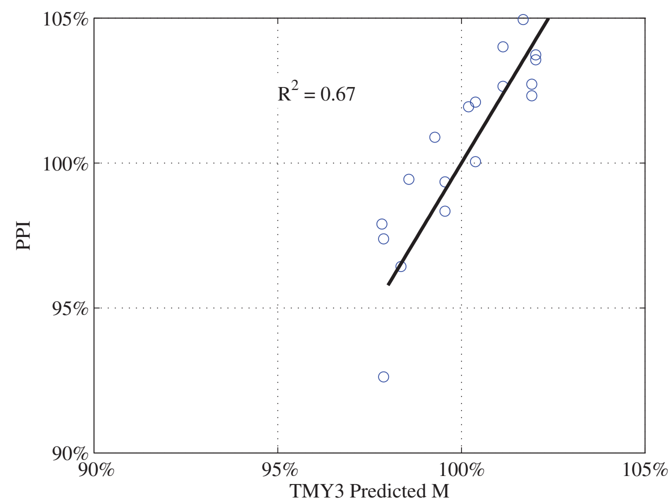

Fig. 5. Comparing TMY-predicted M with the PPI of a multimegawatt CdTe PV system in a temperate climate.

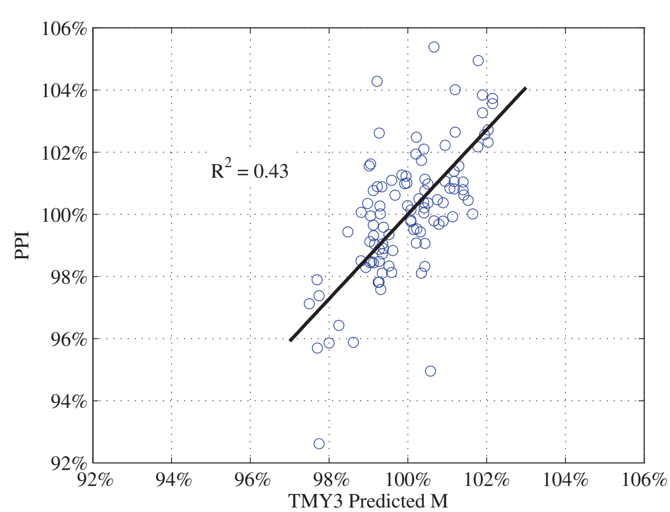

Fig. 6. Comparing TMY-predicted M with the PPI of multiple utility-scale CdTe PV systems in four different climates in North America.

to spectral changes due to atmospheric water absorption because it encompasses the first two major water absorption bands (see Fig. 1). The same is true for homogeneous single-junction copper–indium gallium–selenide, which has a lower spectral sensitivity of 300 nm and an upper limit of between 1100 and 1500 nm, depending on relative concentration of indium and gallium. Similar to CdTe, single-junction amorphous silicon (a-Si) will likely be sensitive to the precipitable water content of the atmosphere as it has a relatively narrow QE (300–700 nm) that does not encompass the major water vapor absorption bands. Additional information about a-Si and c-Si spectral sensitivities to atmospheric water content can be found in [18].

V. Cadmium Telluride Photovoltaic System Performance and M

A multimegawatt CdTe PV system in a temperate climate is monitored by First Solar using a metric which is called the power performance index (PPI). The PPI is a metric representative of system power under standard test conditions of 1000 W/m^2 and 25 °C and is, therefore, insensitive to fluctuations in module temperature and irradiance [6]. The PPI is calculated by regressing temperature-corrected dc power against plane-of-array irradiance measured by a broadband pyranometer. Despite the irradiance and temperature normalization, significant seasonality is observed in the PPI of this system, with diminished performance in the winter, and improved performance in the summer (see Fig. 4). The SMARTS model was run using a nearby TMY3 file to derive the necessary inputs to (2) as described in the previous sections of this paper. M predicted by SMARTS has a similar trend to that observed in the PPI, with performance that varies from 2.1% below nameplate in the winter to 2.4% above nameplate in the summer. In aggregate, the SMARTS model predicts an annual irradiance-weighted spectral shift factor of 100.9% for this location. The trend of lower performance due to a CdTe-disadvantaged spectrum in the winter and higher performance due to CdTe-advantaged spectrum in the summer was previously observed in [16].

Correlating the SMARTS-predicted M and the PPI for this PV plant shows a good relationship (see Fig. 5). One outlier data point of unknown origin does exist. Including this data point in a linear fit yields a coefficient of determination of 0.67. Excluding this outlier data point yields a coefficient of determination of 0.78. While the PPI is generally self-filtering for outages and snow, it is probable that not all timestamps with snow cover were properly filtered, since snowstorms occurred for 24 out of the 31 days in the area in December 2010. This would account for the outlier data point that occurs in this month.

The methodology presented previously was applied to four utility-scale PV systems with dc nameplates totaling more than 100 MW in four different North American climates. The correlation between TMY3/SMARTS-predicted M and measured PV plant PPI on aggregate is weaker than for each individual site studied, but a clear trend is evident (see Fig. 6). Some of the scatter results from the use of a multiyear average TMY3 data as a proxy for measured meteorological inputs into the SMARTS model. The standard deviation of the residuals of a linear fit is 1.8%.

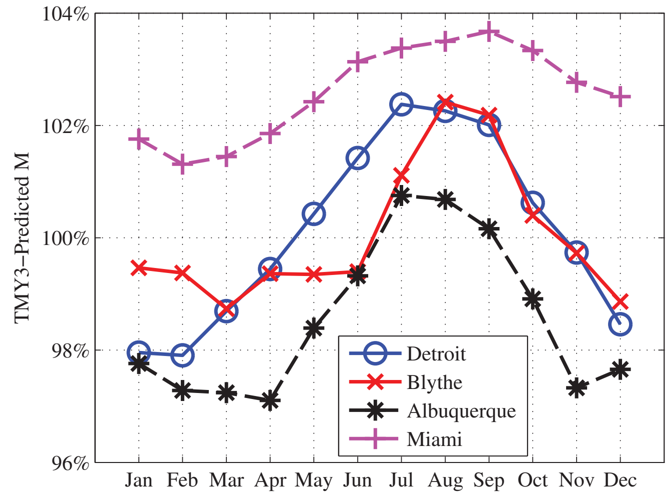

Fig. 7. TMY3-predicted CdTe M in different climates.

TABLE II
Annual Spectral Shift Factors by Location

Location	Annual M
Detroit, MI	100.9%
Las Animas, CO	99.2%
Blythe, CA	100.2%
Las Vegas, NV	99.2%
El Paso, TX	99.4%
Phoenix, AZ	99.5%
San Antonio, TX	101.8%
Lancaster, CA	99.4%
Miami, FL	102.6%
Albuquerque, NM	98.9%
Massena, NY	100.6%

VI. Predicted M for Various Climates

Spectral shift factors for CdTe were calculated using the SMARTS model for 11 locations in the U.S. In general, the temperate climates that were investigated (Massena, NY and Detroit, MI) tended to have a different shape than all others, with larger swings between the winter and summer, and a more symmetrical shape. All sites that were investigated saw enhanced performance in the July through September timeframe when compared with ASTM G173 (nameplate) due to increased precipitable water content of the atmosphere. Similarly, all systems that were investigated saw diminished performance of varying severity when compared with ASTM G173 in the December through March timeframe due to diminished atmospheric water content. Fig. 7 shows the trend of a few sample climates that were investigated using this methodology. Notice the slightly different shapes of the temperate (Detroit) and desert southwest (Blythe) climates. These results suggest that one can expect improved performance of CdTe PV systems in the late summer and early fall during times of high energy demand.

Annual irradiance-weighted values of M were calculated for each of the sites that are investigated and listed in Table II. This

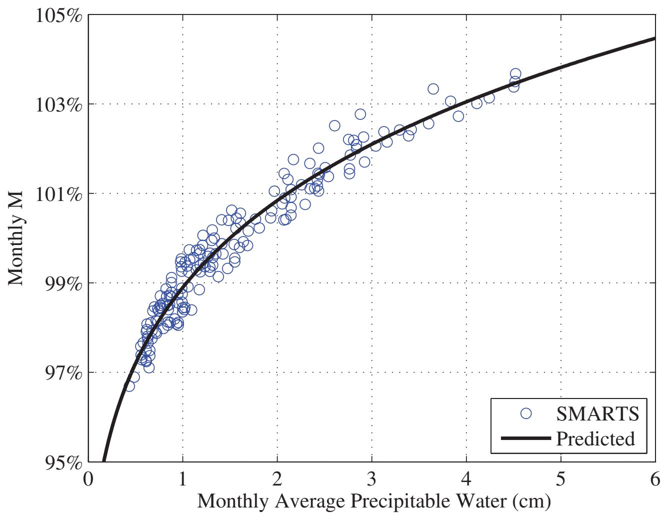

Fig. 8. Monthly SMARTS-predicted M as a function of precipitable water in 11 different North American locations.

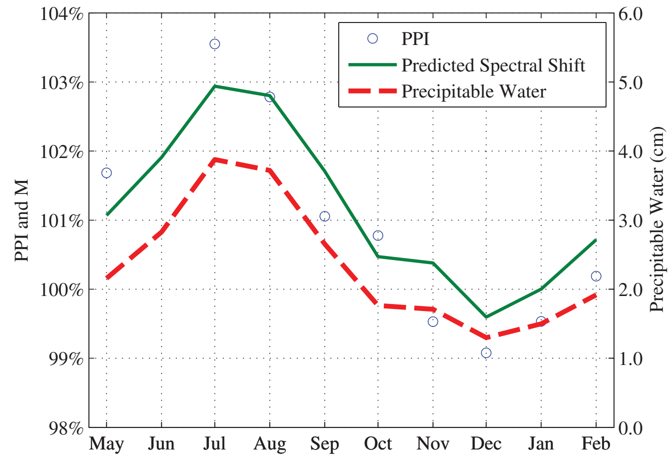

Fig. 9. Monthly average PPI for a multimegawatt CdTe PV system with measured precipitable water and M approximated using (3).

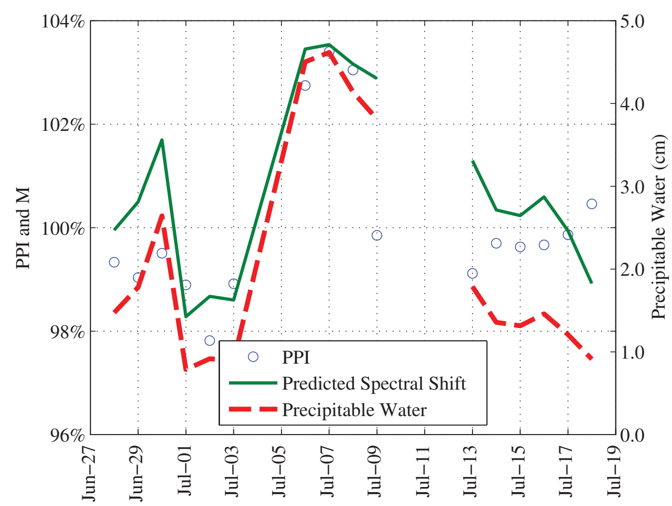

Fig. 10. Measured precipitable water, predicted M, and CdTe system PPI during a thunderstorm in the desert southwest U.S.

shows that on average the magnitude of the annual shift in the spectrum is less than 1% except in the relatively high humidity environments, where CdTe power plants will perform slightly better than predicted without a spectral correction. In all cases, the intraannual uncertainty will be reduced when including a spectral correction in the energy prediction.

VII. Parameterizing Spectral Shift as a Function of Precipitable Water

The previously described sensitivity analysis showed that the predicted monthly M was significantly more sensitive to the precipitable water input than any of the other inputs. Fig. 8 shows the SMARTS calculated monthly M with their respective average precipitable water inputs (from TMY3 data) for all 11 locations that are studied. Recall that ASTM G173 is defined at a precipitable water content of 1.42 cm, and consequently, the correlation predicts a spectral shift of 100% at that value.

The strong correlation between this single-input variable of monthly precipitable water and the calculated M, despite a number of other independent variables, would suggest that M can be approximated for an arbitrary CdTe PV system in a given location, assuming that some information was available about precipitable water by using (3). This correlation was derived by fitting an exponential form to the data shown in Fig. 8 and is represented by the "predicted" line

$$M_{\mathrm{CdTe}} \approx 0.632 + 0.134 \cdot \exp(0.976(P_{\mathrm{wat}} + 0.05)^{0.079}) \quad (3)$$

where precipitable water is defined in units of centimeters. Two reasonable sources of precipitable water are the TMY multiyear averages previously referenced and real-time measured precipitable water data which are publically available for many locations in the U.S. and worldwide from [9] and [10]. Precipitable water can also be reasonably approximated using relative humidity and ambient temperature [15].

The utility of (3) was validated using measured power plant and meteorological data. Measured precipitable water data were downloaded from [9] for a humid location in which a multimegawatt CdTe PV plant was installed. Monthly spectral shift factors were predicted using (2) with the measured precipitable water as inputs. The PPI for the multimegawatt system was also calculated. Both metrics were aggregated into monthly averages and are plotted in Fig. 9.

The correlation between the CdTe PV system PPI and the precipitable water-approximated M is very strong, with a standard deviation of fit residuals of 0.8% and a coefficient of determination of 0.9.

VIII. Short Time-Scale Spectrum Shifts

A large thunderstorm passed over a multimegawatt PV power plant in the desert southwest U.S. in early July 2011. An increase in the PPI of approximately 4% was observed during this timeframe. Measured precipitable water was downloaded for the date range of interest, and the spectral shift factor was approximated using (3). Note the large swings in precipitable water and PPI that occur during the thunderstorm period (see Fig. 10).

The predicted spectral shift factor and measured system PPI are well correlated during the days leading up to and during the thunderstorm (June 26, 2011–July 12, 2011). Data after July 12, 2011, were excluded from the correlation because the system was washed by the rain that occurred during the thunderstorm. The change in soiling rate that occurred during the washing may be confounding the spectral correlation from before to after the thunderstorm. The coefficient of determination of the correlation between M and PPI is 0.8 in this instance.

IX. Conclusion

The data and analyses presented in this paper have demonstrated that variations in atmosphere composition significantly affect the performance of CdTe PV systems when compared with broadband irradiance sensors due to changes in the wavelength at which irradiance is available. Performance data from installed systems suggest that spectral shift factors can be reasonably predicted using TMY3 data as an input to the SMARTS model. Sensitivity analyses demonstrate that precipitable water is the dominant parameter when determining spectral shift factors for a CdTe PV system, and the spectral shift factor was shown to be reasonably approximated by an exponential function of precipitable water. Spectral shift factors that are predicted using both the more complex SMARTS model with TMY3 data as input and the precipitable water approximation with measured data input are shown to be correlated with the power performance of large CdTe PV systems. Future efforts will be focused on incorporating these results into energy predictions at First Solar to lower prediction uncertainty and utilizing the methodology presented to improve performance analysis and characterization techniques.

References

[1] D. L. King, W. E. Boyson, and J. A. Kratochvil, “Analysis of factors influencing the annual energy production of photovoltaic systems,” *Appl. Phys. Lett.*, vol. 44, pp. 432–434, 2002.

[2] C. Gueymard, “Parameterized transmittance model for direct beam and circumsolar spectral irradiance,” *Sol. Energy*, vol. 71, no. 5, pp. 325–346, 2001.

[3] C. Gueymard, “SMARTS, a simple model of the atmospheric radiative transfer of sunshine: Algorithms and performance assessment” Florida Sol. Energy Center, Cocoa, FL, Tech. Rep. FSEC-PF-270-95, 1995.

[4] Nat. Renewable Energy Lab., Golden, CO. *Reference solar spectral irradiance: ASTM G-173* (2012). [Online]. Available: http://rredc.nrel.gov/solar/spectra/am1.5/ASTMG173/ASTMG173.html

[5] S. Wilcox and W. Marion, “User’s manual for TMY3 data sets,” Nat. Renewable Energy Lab., Golden, CO, Tech. Rep. NEWL/TP-581-43156, Apr. 2008.

[6] L. Nelson and C. Hansen, “Evaluation of photovoltaic system power rating methods for a cadmium telluride array,” in *Proc. IEEE Photovoltaic Spec. Conf.*, June 2001.

[7] N. E. Dorsey, *Properties of Ordinary Water-Substance*. New York: Reinhold, 1940, pp. 128–129.

[8] R. G. Eldridge, “Water vapor absorption of visible and near infrared radiation,” *Appl. Opt.*, vol. 6, no. 4, pp. 709–714, 1967.

[9] Univ. Corporation for Atmospheric Res., Boulder, CO, (2011). [Online]. Available: http://www.suominet.ucar.edu/index.html

[10] NASA, Washington, DC. (2012). *Aeronet: Aerosol robotic network* [Online]. Available: http://aeronet.gsfc.nasa.gov/

[11] PVsyst (2012). [Online]. Available: http://www.pvsyst.com/

[12] The Solar Design Company, PV*SOL, Powys, U.K. (2012). [Online]. Available: http://www.solardesign.co.uk/pv.php

[13] Nat. Renewable Energy Lab., Golden, CO. *System advisor model (SAM)* (2012). [Online]. Available: https://sam.nrel.gov/

[14] K. Emery and C. Osterwald, “Measurement of photovoltaic device current as a function of voltage, temperature, intensity and spectrum,” *Sol. Cells*, vol. 21, pp. 313–327, Jun.-Aug. 1987.

[15] W. M. Keogh and A. W. Blakers, “Accurate measurement, using natural sunlight, of silicon solar cells,” *Prog. Photovolt: Res. Appl.*, vol. 12, pp. 1–19, 2004.

[16] R. Gottschalg, D. J. Infield, and M. J. Kearney, “Experimental study of variations of the solar spectrum of relevance to thin film solar cells,” *Sol. Energy Mater. Sol. Cells*, vol. 79, pp. 527–537, 2003.

[17] K. Emery, “Photovoltaic efficiency measurements,” *Proc. SPIE, Organic Photovoltaics V*, vol. 5520, p. 36, 2004.

[18] C. Osterwald, “Calculated solar cell ISC sensitivity to atmospheric conditions under direct and global irradiance,” in *Proc. 18th IEEE Photovoltaic Spec. Conf.*, 1985, pp. 951–956.

Authors’ photographs and biographies not available at the time of publication.